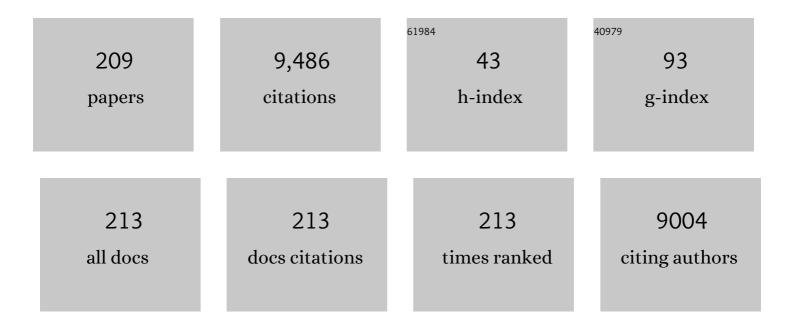
List of Publications by Year in descending order

Source: https://exaly.com/author-pdf/7359734/publications.pdf Version: 2024-02-01



#	Article	IF	CITATIONS
1	Emergent interface vibrational structure of oxide superlattices. Nature, 2022, 601, 556-561.	27.8	40
2	Hyperbolic shear polaritons in low-symmetry crystals. Nature, 2022, 602, 595-600.	27.8	78
3	Anisotropy and Modal Hybridization in Infrared Nanophotonics Using Low-Symmetry Materials. ACS Photonics, 2022, 9, 1078-1095.	6.6	18
4	Long-wave infrared super-resolution wide-field microscopy using sum-frequency generation. Applied Physics Letters, 2022, 120, 131102.	3.3	3
5	Collective Phonon–Polaritonic Modes in Silicon Carbide Subarrays. ACS Nano, 2022, 16, 963-973.	14.6	6
6	Manipulating polaritons at the extreme scale in van der Waals materials. Nature Reviews Physics, 2022, 4, 578-594.	26.6	51
7	Long-lived modulation of plasmonic absorption by ballistic thermal injection. Nature Nanotechnology, 2021, 16, 47-51.	31.5	40
8	Ultrastrong plasmon–phonon coupling via epsilon-near-zero nanocavities. Nature Photonics, 2021, 15, 125-130.	31.4	78
9	Nanoscale Spectroscopy of Dielectric Properties of Mica. ACS Photonics, 2021, 8, 175-181.	6.6	16
10	Filterless Nondispersive Infrared Sensing using Narrowband Infrared Emitting Metamaterials. ACS Photonics, 2021, 8, 472-480.	6.6	20
11	Guided Mid″R and Near″R Light within a Hybrid Hyperbolicâ€Material/Silicon Waveguide Heterostructure. Advanced Materials, 2021, 33, e2004305.	21.0	20
12	Engineering the Spectral and Spatial Dispersion of Thermal Emission via Polariton–Phonon Strong Coupling. Nano Letters, 2021, 21, 1831-1838.	9.1	44
13	Mid-wave to near-IR optoelectronic properties and epsilon-near-zero behavior in indium-doped cadmium oxide. Physical Review Materials, 2021, 5, .	2.4	12
14	Hybrid Waveguides: Guided Midâ€iR and Nearâ€iR Light within a Hybrid Hyperbolicâ€Material/Silicon Waveguide Heterostructure (Adv. Mater. 11/2021). Advanced Materials, 2021, 33, 2170079.	21.0	0
15	Multi-frequency coherent emission from superstructure thermal emitters. Applied Physics Letters, 2021, 118, .	3.3	7
16	Van der Waals Phonon Polariton Microstructures for Configurable Infrared Electromagnetic Field Localizations. Advanced Science, 2021, 8, 2004872.	11.2	20
17	Long-Lived Phonon Polaritons in Hyperbolic Materials. Nano Letters, 2021, 21, 5767-5773.	9.1	38
18	Ultrahigh-Resolution, Label-Free Hyperlens Imaging in the Mid-IR. Nano Letters, 2021, 21, 7921-7928.	9.1	17

#	Article	IF	CITATIONS
19	Experimental confirmation of long hyperbolic polariton lifetimes in monoisotopic (10B) hexagonal boron nitride at room temperature. APL Materials, 2021, 9, .	5.1	16
20	Enhanced Absorption with Graphene-Coated Silicon Carbide Nanowires for Mid-Infrared Nanophotonics. Nanomaterials, 2021, 11, 2339.	4.1	7
21	Interface quality in GaSb/AlSb short period superlattices. Journal of Vacuum Science and Technology A: Vacuum, Surfaces and Films, 2021, 39, .	2.1	4
22	Deterministic inverse design of Tamm plasmon thermal emitters with multi-resonant control. Nature Materials, 2021, 20, 1663-1669.	27.5	46
23	Phonon engineering of boron nitride via isotopic enrichment. Journal of Materials Research, 2021, 36, 4394-4403.	2.6	8
24	Ultrafast Active Tuning of the Berreman Mode. ACS Photonics, 2020, 7, 279-287.	6.6	14
25	Nearâ€Unity and Narrowband Thermal Emissivity in Balanced Dielectric Metasurfaces. Advanced Optical Materials, 2020, 8, 1901470.	7.3	37
26	Van der Waals Semiconductors: Infrared Permittivity of the Biaxial van der Waals Semiconductor αâ€MoO <sub>3</sub> from Near―and Farâ€Field Correlative Studies (Adv. Mater. 29/2020). Advanced Materials, 2020, 32, 2070220.	21.0	5
27	Image polaritons in boron nitride for extreme polariton confinement with low losses. Nature Communications, 2020, 11, 3649.	12.8	56
28	Lithography-free IR polarization converters via orthogonal in-plane phonons in α-MoO3 flakes. Nature Communications, 2020, 11, 5771.	12.8	54
29	Narrowband Polaritonic Thermal Emitters Driven by Waste Heat. ACS Omega, 2020, 5, 10900-10908.	3.5	34
30	Towards low- loss on-chip nanophotonics with coupled graphene and silicon carbide: a review. JPhys Materials, 2020, 3, 032005.	4.2	15
31	Infrared Permittivity of the Biaxial van der Waals Semiconductor αâ€MoO <sub>3</sub> from Near―and Farâ€Field Correlative Studies. Advanced Materials, 2020, 32, e1908176.	21.0	99
32	Exploiting Phononâ€Resonant Nearâ€Field Interaction for the Nanoscale Investigation of Extended Defects. Advanced Functional Materials, 2020, 30, 1907357.	14.9	12
33	Vibrational Coupling to Epsilon-Near-Zero Waveguide Modes. ACS Photonics, 2020, 7, 614-621.	6.6	35
34	Ultraviolet to far-infrared dielectric function of <mml:math xmlns:mml="http://www.w3.org/1998/Math/MathML"&gt;<mml:mrow><mml:mi>n</mml:mi></mml:mrow>-doped cadmium oxide thin films. Physical Review Materials, 2020, 4, .</mml:math 	nath4	16
35	High-Q dark hyperbolic phonon-polaritons in hexagonal boron nitride nanostructures. Nanophotonics, 2020, 9, 1457-1467.	6.0	13
36	Enhanced Mid -Infrared Reflectance with Graphene Coated Silicon Carbide Nanowires. , 2020, , .		0

#	Article	IF	CITATIONS
37	Electrically defined topological interface states of graphene surface plasmons based on a gate-tunable quantum Bragg grating. Nanophotonics, 2019, 8, 1417-1431.	6.0	8
38	Photonics with hexagonal boron nitride. Nature Reviews Materials, 2019, 4, 552-567.	48.7	504
39	Refractive Index-Based Control of Hyperbolic Phonon-Polariton Propagation. Nano Letters, 2019, 19, 7725-7734.	9.1	69
40	Surface Phonon Polariton Resonance Imaging Using Long-Wave Infrared-Visible Sum-Frequency Generation Microscopy. ACS Photonics, 2019, 6, 3017-3023.	6.6	14
41	Ultralow Loss Polaritons in Isotopically Pure Hexagonal Boron Nitride. , 2019, , .		0
42	Rapid Bimolecular and Defect-Assisted Carrier Recombination in Hexagonal Boron Nitride. Journal of Physical Chemistry C, 2019, 123, 14689-14695.	3.1	2
43	Controlling the Infrared Dielectric Function through Atomic-Scale Heterostructures. ACS Nano, 2019, 13, 6730-6741.	14.6	33
44	Second Harmonic Generation from Phononic Epsilon-Near-Zero Berreman Modes in Ultrathin Polar Crystal Films. ACS Photonics, 2019, 6, 1365-1371.	6.6	42
45	Probing polaritons in the mid- to far-infrared. Journal of Applied Physics, 2019, 125, .	2.5	48
46	Hybrid longitudinal-transverse phonon polaritons. Nature Communications, 2019, 10, 1682.	12.8	46
47	Influence of spatial dispersion on spectral tuning of phonon-polaritons. Physical Review B, 2019, 100, .	3.2	5
48	Polaritonic Hybrid-Epsilon-near-Zero Modes: Beating the Plasmonic Confinement vs Propagation-Length Trade-Off with Doped Cadmium Oxide Bilayers. Nano Letters, 2019, 19, 948-957.	9.1	61
49	Polaritonic hybrid-epsilon-near-zero modes: engineering strong optoelectronic coupling and dispersion in doped cadmium oxide bilayers (Conference Presentation). , 2019, , .		1
50	(Invited) Controlling Light with Phonons in Polar Semiconductors: Novel Approaches to Infrared Nanophotonics. ECS Meeting Abstracts, 2019, , .	0.0	0
51	Fabrication of phonon-based metamaterial structures using focused ion beam patterning. Applied Physics Letters, 2018, 112, .	3.3	10
52	High-Contrast Infrared Absorption Spectroscopy via Mass-Produced Coaxial Zero-Mode Resonators with Sub-10 nm Gaps. Nano Letters, 2018, 18, 1930-1936.	9.1	88
53	Nanoscale Mapping and Spectroscopy of Nonradiative Hyperbolic Modes in Hexagonal Boron Nitride Nanostructures. Nano Letters, 2018, 18, 1628-1636.	9.1	55
54	Active tuning of surface phonon polariton resonances via carrier photoinjection. Nature Photonics, 2018, 12, 50-56.	31.4	102

#	Article	IF	CITATIONS
55	Ultralow-loss polaritons in isotopically pure boronÂnitride. Nature Materials, 2018, 17, 134-139.	27.5	291
56	Approaches for Dynamic IR N ano-Optics using 2D Materials. , 2018, , .		0
57	Implementation of plasmonic band structure to understand polariton hybridization within metamaterials. Optics Express, 2018, 26, 29363.	3.4	4
58	Probing hyperbolic polaritons using infrared attenuated total reflectance micro-spectroscopy. MRS Communications, 2018, 8, 1418-1425.	1.8	17
59	Strong Coupling Effects Between IR-Inactive Zone Folded LO Phonon and Localized Surface Phonon Polariton Modes in SiC Nanopillars. NATO Science for Peace and Security Series B: Physics and Biophysics, 2018, , 417-418.	0.3	0
60	Precise control of infrared polarization using crystal vibrations. Nature, 2018, 562, 499-501.	27.8	24
61	Reconfigurable infrared hyperbolic metasurfaces using phase change materials. Nature Communications, 2018, 9, 4371.	12.8	148
62	Chapter 12 Semiconductor Nanophotonics Using Surface Polaritons. NATO Science for Peace and Security Series B: Physics and Biophysics, 2018, , 235-254.	0.3	1
63	Strong confinement of optical fields using localized surface phonon polaritons in cubic boron nitride. Optics Letters, 2018, 43, 2177.	3.3	17
64	Theoretical analysis of graphene plasmon cavities. Applied Materials Today, 2018, 12, 283-293.	4.3	12
65	Sub-nanometer Thin Oxide Film Sensing with Localized Surface Phonon Polaritons. ACS Photonics, 2018, 5, 2807-2815.	6.6	52
66	Strong Coupling of Epsilon-Near-Zero Phonon Polaritons in Polar Dielectric Heterostructures. Nano Letters, 2018, 18, 4285-4292.	9.1	71
67	Interactions of Hexagonal Boron Nitride with the Insulator-Metal Phase Transition of Vanadium Dioxide. , 2018, , .		0
68	Symmetry Breaking and Active Fano Resonance Tuning in Dolmen Nanostructures. NATO Science for Peace and Security Series B: Physics and Biophysics, 2018, , 407-408.	0.3	0
69	Surface-Enhanced Infrared Absorption Spectroscopy via Coaxial Zero-Mode Resonators with Sub-10-nm Gaps. , 2018, , .		0
70	High-Order Multipole Resonances in Cuboidal Surface Phonon Polariton Nanoresonators. NATO Science for Peace and Security Series B: Physics and Biophysics, 2017, , 501-502.	0.3	0
71	Phonon-Polaritonic Bowtie Nanoantennas: Controlling Infrared Thermal Radiation at the Nanoscale. ACS Photonics, 2017, 4, 1753-1760.	6.6	114
72	Graphene Plasmon Cavities Made with Silicon Carbide. ACS Omega, 2017, 2, 3640-3646.	3.5	35

#	Article	IF	CITATIONS
73	Polaritons in layered two-dimensional materials. Nature Materials, 2017, 16, 182-194.	27.5	963
74	Multi-resonant Metamaterials for Visible and Near-IR Frequencies. NATO Science for Peace and Security Series B: Physics and Biophysics, 2017, , 555-555.	0.3	0
75	Ultrafast carrier dynamics in wide bandgap semiconductor materials. , 2017, , .		0
76	Low-Loss Phonon Polaritons in Nanostructured Dielectrics. NATO Science for Peace and Security Series B: Physics and Biophysics, 2017, , 511-512.	0.3	0
77	Experimental demonstration of the optical lattice resonance in arrays of Si nanoresonators. Applied Physics Letters, 2016, 108, .	3.3	26
78	Imaging of Anomalous Internal Reflections of Hyperbolic Phonon-Polaritons in Hexagonal Boron Nitride. Nano Letters, 2016, 16, 3858-3865.	9.1	106
79	Two-dimensional gallium nitride realized via grapheneÂencapsulation. Nature Materials, 2016, 15, 1166-1171.	27.5	626
80	Photoinduced tunability of the reststrahlen band in <mml:math xmlns:mml="http://www.w3.org/1998/Math/MathML"&gt;<mml:mn>4</mml:mn><mml:mi>H</mml:mi><mml:mo> Physical Review B, 2016, 93, .</mml:mo></mml:math 	â <b>^' s/@</b> nml:n	no <b>37</b> mml:mi>
81	Resonant Enhancement of Second-Harmonic Generation in the Mid-Infrared Using Localized Surface Phonon Polaritons in Subdiffractional Nanostructures. Nano Letters, 2016, 16, 6954-6959.	9.1	53
82	Aspect-ratio driven evolution of high-order resonant modes and near-field distributions in localized surface phonon polariton nanostructures. Scientific Reports, 2016, 6, 32959.	3.3	25
83	Role of epsilon-near-zero substrates in the optical response of plasmonic antennas. Optica, 2016, 3, 339.	9.3	162
84	Atomic-scale photonic hybrids for mid-infrared and terahertz nanophotonics. Nature Nanotechnology, 2016, 11, 9-15.	31.5	136
85	Mid-Infrared Second Harmonic Spectroscopy Probing Surface Phonon Polariton Localization in SiC Nanopillars. , 2016, , .		0
86	Perfect interferenceless absorption at infrared frequencies by a van der Waals crystal. Physical Review B, 2015, 92, .	3.2	51
87	Nanotubes, nanobelts, nanowires, and nanorods of silicon carbide from the wheat husks. Journal of Applied Physics, 2015, 118, 104904.	2.5	21
88	Resonance spectra of diabolo optical antenna arrays. AIP Advances, 2015, 5, 107149.	1.3	3
89	Low-loss, infrared and terahertz nanophotonics using surface phonon polaritons. Nanophotonics, 2015, 4, 44-68.	6.0	547
90	Understanding carrier injection effects upon the Reststrahlen band of SiC using transient infrared spectroscopy (Presentation Recording). Proceedings of SPIE, 2015, , .	0.8	0

#	Article	IF	CITATIONS
91	Hyperbolic phonon-polaritons in boron nitride for near-field optical imaging and focusing. Nature Communications, 2015, 6, 7507.	12.8	399
92	Mid-infrared nanophotonics. Nature Materials, 2015, 14, 364-366.	27.5	57
93	Nanoparticles and nanorods of silicon carbide from the residues of corn. Journal of Applied Physics, 2015, 117, .	2.5	21
94	Probing hyperbolic polaritons. Nature Photonics, 2015, 9, 638-640.	31.4	11
95	Towards low-loss, infrared and THz nanophotonics and metamaterials: surface phonon polariton modes in polar dielectric crystals (Presentation Recording). , 2015, , .		0
96	Sub-diffractional, volume-confined polaritons in a natural hyperbolic material: hexagonal boron nitride (Presentation Recording). , 2015, , .		0
97	Etch free graphene transfer to polymers. Surface and Coatings Technology, 2014, 241, 118-122.	4.8	10
98	Sub-diffractional volume-confined polaritons in the natural hyperbolic material hexagonal boron nitride. Nature Communications, 2014, 5, 5221.	12.8	686
99	Spectral Tuning of Localized Surface Phonon Polariton Resonators for Low-Loss Mid-IR Applications. ACS Photonics, 2014, 1, 718-724.	6.6	134
100	Focused Ion Beam Direct Write Nanofabrication of Surface Phonon Polariton Metamaterial Nanostructures. Microscopy and Microanalysis, 2014, 20, 358-359.	0.4	2
101	Enhanced plasmon resonance and light absorption in diabolo metal bar optical antennas. , 2014, , .		0
102	Low-Loss, Extreme Subdiffraction Photon Confinement via Silicon Carbide Localized Surface Phonon Polariton Resonators. Nano Letters, 2013, 13, 3690-3697.	9.1	259
103	Formation of Nanodimensional 3C-SiC Structures from Rice Husks. Journal of Electronic Materials, 2013, 42, 799-804.	2.2	18
104	Large surface-enhanced Raman scattering from self-assembled gold nanosphere monolayers. Applied Physics Letters, 2013, 102, .	3.3	38
105	Production of nanoscale particles and nanorods of SiC from sorghum leaves. Industrial Crops and Products, 2013, 51, 158-162.	5.2	18
106	Controlling the local chemical reactivity of graphene through spatial functionalization. Carbon, 2013, 60, 84-93.	10.3	32
107	Chemical Gradients on Graphene To Drive Droplet Motion. ACS Nano, 2013, 7, 4746-4755.	14.6	142
108	Plasmon drag effect in metal nanostructures. New Journal of Physics, 2013, 15, 113061.	2.9	49

#	Article	IF	CITATIONS
109	Experimental evidence for mobile luminescence center mobility on partial dislocations in 4H-SiC using hyperspectral electroluminescence imaging. Applied Physics Letters, 2013, 102, .	3.3	10
110	Mie resonance-enhanced light absorption in periodic silicon nanopillar arrays. Optics Express, 2013, 21, 27587.	3.4	117
111	Plasmon Drag Effect in Metal Nanostructures. , 2013, , .		0
112	Growth of Vertically Aligned ZnO Nanowire Arrays Using Bilayered Metal Catalysts. Journal of Nanomaterials, 2012, 2012, 1-7.	2.7	6
113	Electrical Characterization of the Graphene-SiC Heterojunction. Materials Science Forum, 2012, 717-720, 641-644.	0.3	0
114	Pitch-dependent resonances and near-field coupling in infrared nanoantenna arrays. Optics Express, 2012, 20, 27725.	3.4	34
115	Microwave-induced transformation of rice husks to SiC. Journal of Applied Physics, 2012, 111, .	2.5	21
116	Mitigating Defects within Silicon Carbide Epitaxy. Journal of the Electrochemical Society, 2012, 159, R46-R51.	2.9	11
117	Spoof-like plasmonic behavior of plasma enhanced atomic layer deposition grown Ag thin films. Applied Physics Letters, 2012, 100, 053106.	3.3	23
118	Bilayer graphene by bonding CVD graphene to epitaxial graphene. Journal of Vacuum Science and Technology B:Nanotechnology and Microelectronics, 2012, 30, 03D110.	1.2	10
119	Recovery of Bipolar-Current Induced Degradations in High-Voltage Implanted-Gate Junction Field Effect Transistors. Materials Science Forum, 2012, 717-720, 1013-1016.	0.3	Ο
120	Reduced Self-Heating in AlGaN/GaN HEMTs Using Nanocrystalline Diamond Heat-Spreading Films. IEEE Electron Device Letters, 2012, 33, 23-25.	3.9	100
121	Correlation of Extended Defects on Carrier Lifetime in Thick SiC Epilayers. Materials Science Forum, 2012, 717-720, 297-300.	0.3	4
122	Investigation of the Epitaxial Graphene/p-SiC Heterojunction. IEEE Electron Device Letters, 2012, 33, 1610-1612.	3.9	12
123	Degradation and Full Recovery in High-Voltage Implanted-Gate SiC JFETs Subjected to Bipolar Current Stress. IEEE Electron Device Letters, 2012, 33, 952-954.	3.9	20
124	Nonâ€lithographic SERS Substrates: Tailoring Surface Chemistry for Au Nanoparticle Cluster Assembly. Small, 2012, 8, 2239-2249.	10.0	68
125	Bilayer Graphene Grown on 4H-SiC (0001) Step-Free Mesas. Nano Letters, 2012, 12, 1749-1756.	9.1	50
126	The Role of Propagating and Localized Surface Plasmons for SERS Enhancement in Periodic Nanostructures. Plasmonics, 2012, 7, 143-150.	3.4	26

#	Article	IF	CITATIONS
127	Temperature profiling in AlGaN/GaN HEMTs with nanocrystalline diamond heat spreading layers by Raman spectroscopy. , 2011, , .		1
128	Quantifying pulsed laser induced damage to graphene. Applied Physics Letters, 2011, 99, .	3.3	133
129	Plasmo-photonic nanopillar array for large-area surface-enhanced Raman scattering sensors. , 2011, , .		Ο
130	Large-area plasmonic hot-spot arrays: sub-2 nm interparticle separations with plasma-enhanced atomic layer deposition of Ag on periodic arrays of Si nanopillars. Optics Express, 2011, 19, 26056.	3.4	51
131	Plasmonically enhanced emission from an inverted GaN light emitting diode. , 2011, , .		0
132	Plasmonic Nanopillar Arrays for Large-Area, High-Enhancement Surface-Enhanced Raman Scattering Sensors. ACS Nano, 2011, 5, 4046-4055.	14.6	197
133	High growth rate 4H-SiC epitaxial growth using dichlorosilane in a hot-wall CVD reactor. Journal of Crystal Growth, 2011, 316, 60-66.	1.5	43
134	Structure and Morphology of Inclusions in 4° Offcut 4H-SiC Epitaxial Layers. Journal of Electronic Materials, 2011, 40, 413-418.	2.2	25
135	Surface Enhanced Raman Scattering Enhancements from Silver Atomic Layer Deposition Coated Nanowire. , 2011, , .		1
136	Extended defects that affect carrier lifetime in high blocking voltage SiC epilayers. , 2011, , .		0
137	Influence of Intercalated Silicon on the Transport Properties of Graphene. Materials Science Forum, 2011, 679-680, 793-796.	0.3	1
138	(Invited) Mitigating Defects within Silicon Carbide Epitaxy. ECS Transactions, 2011, 41, 261-271.	0.5	1
139	Below Bandgap Excitation of SnO2 Nanowires: The Relaxation of Trap States. , 2011, , .		1
140	Epitaxial graphene: dry transfer and materials characterization. Proceedings of SPIE, 2010, , .	0.8	0
141	Surface modification of metal and metal coated nanoparticles to induce clustering. , 2010, , .		0
142	Diffraction Contrast of Threading Dislocations in GaN and 4H-SiC Epitaxial Layers Using Electron Channeling Contrast Imaging. Journal of Electronic Materials, 2010, 39, 743-746.	2.2	5
143	Electrical and Optical Characterization of AlGaN/GaN HEMTs with InÂSitu and ExÂSitu Deposited SiN x Layers. Journal of Electronic Materials, 2010, 39, 2452-2458.	2.2	27
144	(Invited) Techniques for the Dry Transfer of Epitaxial Graphene onto Arbitrary Substrates. ECS Transactions, 2010, 33, 177-186.	0.5	1

#	Article	IF	CITATIONS
145	Cysteamine coated Ag and Au nanorods for improved surface enhanced Raman scattering from dinitrotoluene and trinitrotoluene. , 2010, , .		0
146	Techniques for the Dry Transfer of Epitaxial Graphene onto Arbitrary Substrates. Materials Science Forum, 2010, 645-648, 633-636.	0.3	2
147	Recent Developments in SiC Homoepitaxy Using Dichlorosilane for High Power Devices. Materials Research Society Symposia Proceedings, 2010, 1246, 1.	0.1	1
148	On the driving force for recombination-induced stacking fault motion in 4H–SiC. Journal of Applied Physics, 2010, 108, .	2.5	80
149	On the high curvature coefficient rectifying behavior of nanocrystalline diamond heterojunctions to 4H-SiC. Applied Physics Letters, 2010, 97, .	3.3	8
150	Investigation of deep levels in nitrogen doped 4H–SiC epitaxial layers grown on 4° and 8° off-axis substrates. Journal of Applied Physics, 2010, 108, 054906.	2.5	6
151	Plasmo-photonic nanowire arrays for large-area surface-enhanced Raman scattering sensors. Proceedings of SPIE, 2010, , .	0.8	2
152	Reduced self-heating in ALGaN/GaN HEMTs using nanocrystalline diamond heat spreading films. , 2010, ,		64
153	Technique for the Dry Transfer of Epitaxial Graphene onto Arbitrary Substrates. ACS Nano, 2010, 4, 1108-1114.	14.6	190
154	Recombination-induced stacking fault degradation of 4H-SiC merged-PiN-Schottky diodes. Journal of Applied Physics, 2009, 106, .	2.5	49
155	On the Driving Force of Shockley Stacking Fault Motion in 4H-SiC. ECS Transactions, 2009, 25, 93-104.	0.5	4
156	Growth and photoluminescence properties of vertically aligned SnO2 nanowires. Journal of Crystal Growth, 2009, 311, 3158-3162.	1.5	31
157	Resistively Detected ESR andÂENDORÂExperiments inÂNarrowÂandÂWideÂQuantumÂWells: AÂComparative Study. Topics in Applied Physics, 2009, , 1-13.	0.8	0
158	Epitaxial SiC Growth Morphology and Extended Defects Investigated by Electron Backscatter Diffraction and Electron Channeling Contrast Imaging. Journal of Electronic Materials, 2008, 37, 691-698.	2.2	11
159	Influence of Temperature on Shockley Stacking Fault Expansion and Contraction in SiC PiN Diodes. Journal of Electronic Materials, 2008, 37, 699-705.	2.2	22
160	Investigation of Electron–Hole Recombination-Activated Partial Dislocations and Their Behavior in 4H-SiC Epitaxial Layers. Journal of Electronic Materials, 2008, 37, 706-712.	2.2	0
161	Design of Gallium Nitride Resonant Cavity Lightâ€Emitting Diodes on Si Substrates. Advanced Materials, 2008, 20, 115-118.	21.0	28
162	Study of triangular defects and inverted pyramids in 4H-SiC 4° off-cut (0001) Si face epilayers. Journal of Crystal Growth, 2008, 310, 4443-4450.	1.5	25

#	Article	IF	CITATIONS
163	Measurement of Local Temperatures Using µ-Raman of SiC and AlGaN-GaN/SiC Power and RF Devices. Materials Science Forum, 2008, 600-603, 1111-1114.	0.3	6
164	Dislocation Nucleation and Growth in MOCVD GaN/AlN Films on Stepped and Step-free 4H-SiC Mesa Substrates. Materials Research Society Symposia Proceedings, 2008, 1090, 52401.	0.1	0
165	Determination of the Core-structure of Shockley Partial Dislocations in 4H-SiC. Materials Research Society Symposia Proceedings, 2008, 1069, 1069-D03-03-01.	0.1	2
166	Infrared PL Signatures of n-Type Bulk SiC Substrates with Nitrogen Impurity Concentration between 10 <sup>16</sup> and 10 <sup>17</sup> cm <sup>-3</sup> . Materials Science Forum, 2008, 600-603, 449-452.	0.3	1
167	Nondestructive defect measurement and surface analysis of 3C-SiC on Si (001) by electron channeling contrast imaging. Materials Research Society Symposia Proceedings, 2008, 1068, 1.	0.1	0
168	Temperature Dependence of Shockley Stacking Fault Expansion and Contraction in 4H-SiC p-i-n Diodes. Materials Science Forum, 2008, 600-603, 273-278.	0.3	1
169	Influence of Shockley Stacking Fault Expansion and Contraction on the Electrical Behavior of 4H-SiC DMOSFETs and MPS diodes. Materials Research Society Symposia Proceedings, 2008, 1069, 1.	0.1	1
170	Integrated Optics Utilizing GaN-Based Layers on Silicon Substrates. Materials Research Society Symposia Proceedings, 2008, 1068, 1.	0.1	1
171	Simulation of Forescattered Electron Channeling Contrast Imaging of Threading Dislocations Penetrating SiC Surfaces. Materials Research Society Symposia Proceedings, 2008, 1068, 1.	0.1	0
172	Influence of Shockley stacking fault propagation and contraction on electrical behavior of 4H-SiC pin diodes and DMOSFETs. , 2007, , .		3
173	Plasmonically enhanced emission from a group-III nitride nanowire emitter. Nanotechnology, 2007, 18, 265401.	2.6	13
174	Electron channeling contrast imaging of atomic steps and threading dislocations in 4H-SiC. Applied Physics Letters, 2007, 90, 234101.	3.3	43
175	Differences in emission spectra of Si- and C-core partial dislocations. Applied Physics Letters, 2007, 90, 153503.	3.3	24
176	Nanocrystalline diamond films as UV-semitransparent Schottky contacts to 4H-SiC. Applied Physics Letters, 2007, 91, .	3.3	20
177	Investigation of nanocrystalline diamond films as UV transparent Ohmic contacts to GaN. , 2007, , .		0
178	Nondestructive analysis of threading dislocations in GaN by electron channeling contrast imaging. Applied Physics Letters, 2007, 91, .	3.3	49
179	Free carrier distribution profiling of 4H-SiC substrates using a commercial optical scanner. Journal of Applied Physics, 2007, 101, 093506.	2.5	18
180	The influence of substrate atomic step morphology on threading dislocation distributions in iii-nitride films. , 2007, , .		1

#	Article	IF	CITATIONS
181	Fabrication of GaN suspended photonic crystal membranes and resonant nanocavities on Si(111). Journal of Vacuum Science & Technology B, 2007, 25, 721.	1.3	16
182	Temperature-mediated saturation and current-induced recovery of the Vf drift in 4H-SiCâ€^p-i-n diodes. Applied Physics Letters, 2007, 91, .	3.3	14
183	Reversal of forward voltage drift in 4H-SiC p-i-n diodes via low temperature annealing. Applied Physics Letters, 2007, 90, 143519.	3.3	46
184	Thermal Annealing and Propagation of Shockley Stacking Faults in 4H-SiC PiN Diodes. Journal of Electronic Materials, 2007, 36, 318-323.	2.2	26
185	Photoluminescence and Electroluminescence Imaging of Carrot Defect in 4H-SiC Epitaxy. Journal of Electronic Materials, 2007, 36, 297-306.	2.2	19
186	Temperature dependence of the resistively detected electron spin resonance signals in a wide parabolic quantum well. AIP Conference Proceedings, 2007, , .	0.4	0
187	Improved ultraviolet emission from reduced defect gallium nitride homojunctions grown on step-free 4H-SiC mesas. Applied Physics Letters, 2006, 88, 263509.	3.3	19
188	Dynamic nuclear polarization and nuclear magnetic resonance in the vicinity of edge states of a 2DES in GaAs quantum wells. Solid State Nuclear Magnetic Resonance, 2006, 29, 52-65.	2.3	5
189	Characterization of defects in the drift region of 4H-SiC pin diodes via optical beam induced current. Journal of Vacuum Science & Technology B, 2006, 24, 2178.	1.3	10
190	Optical, Electrical and Lifetime Characterization of In-Grown Stacking Faults in 4H-SiC. Materials Research Society Symposia Proceedings, 2006, 911, 5.	0.1	0
191	SiC Substrate Doping Profiles Using Commercial Optical Scanners. Materials Science Forum, 2006, 527-529, 725-728.	0.3	2
192	Observation of Free Carrier Redistribution Resulting from Stacking Fault Formation in Annealed 4H-SiC. Materials Science Forum, 2006, 527-529, 347-350.	0.3	9
193	Non-Destructive Electro- and Photo-Luminescence Imaging of Dislocations in SiC Epitaxy. Materials Research Society Symposia Proceedings, 2006, 911, 3.	0.1	1
194	Observation of a multilayer planar in-grown stacking fault in 4H-SiC p-i-n diodes. Applied Physics Letters, 2006, 89, 103519.	3.3	18
195	MD-ENDOR Spectroscopy in a Two-Dimensional Electron System in the Regime of the Quantum Hall Effect. AIP Conference Proceedings, 2005, , .	0.4	0
196	Electron spin resonance in a wide parabolic quantum well. Physical Review B, 2005, 72, .	3.2	8
197	Temperature dependence of electrically detected ESR at filling factor ν=1 in a 2DEG. Physica E: Low-Dimensional Systems and Nanostructures, 2003, 17, 320-321.	2.7	0
198	Temperature dependence and mechanism of electrically detected ESR at theî½=1filling factor of a two-dimensional electron system. Physical Review B, 2003, 67, .	3.2	20

#	Article	IF	CITATIONS
199	Impact of 4H-SiC Substrate Defectivity on Epilayer Injected Carrier Lifetimes. Materials Science Forum, 0, 600-603, 481-484.	0.3	6
200	Synchrotron X-Ray Topographic Studies of Recombination Activated Shockley Partial Dislocations in 4H-Silicon Carbide Epitaxial Layers. Materials Science Forum, 0, 600-603, 357-360.	0.3	2
201	Variations in the Measured Carrier Lifetimes of n <sup>-</sup> 4H-SiC Epilayers. Materials Science Forum, 0, 600-603, 489-492.	0.3	0
202	Differences in Emission Spectra of Dislocations in 4H-SiC Epitaxial Layers. Materials Science Forum, 0, 600-603, 345-348.	0.3	21
203	Effect of Bipolar Gate-to-Drain Current on the Electrical Properties of Vertical Junction Field Effect Transistors. Materials Science Forum, 0, 615-617, 719-722.	0.3	8
204	Long Carrier Lifetime in 4H-SiC Epilayers Using Chlorinated Precursors. Materials Science Forum, 0, 615-617, 291-294.	0.3	7
205	On the Luminescence and Driving Force of Stacking Faults in 4H-SiC. Materials Science Forum, 0, 645-648, 277-282.	0.3	4
206	9 kV, 1 cm <sup>2</sup> SiC Gate Turn-Off Thyristors. Materials Science Forum, 0, 645-648, 1017-1020.	0.3	23
207	Growth of 4H- and 3C-SiC Epitaxial Layers on 4H-SiC Step-Free Mesas. Materials Science Forum, 0, 679-680, 119-122.	0.3	1
208	Luminescence Imaging of Extended Defects in SiC via Hyperspectral Imaging. Materials Science Forum, 0, 717-720, 403-406.	0.3	2
209	Ultraviolet Photoluminescence Imaging of Stacking Fault Contraction in 4H-SiC Epitaxial Layers. Materials Science Forum. 0, 717-720, 391-394.	0.3	9